Principle of extreme energy cosmic ray observation in the JEM-EUSO Mission

K. Shinozaki*, J. Szabelski † and T. Wibig †, for JEM-EUSO Collaboration
* *RIKEN, 2-1 Hirosawa, 351-0198 Wako, Japan*
† *Andrzej Soltan Institute for Nuclear Studies, PL-90-950 Łódź, Poland*

***Abstract*. JEM-EUSO is the innovative extreme energy cosmic ray (EECR) observation mission based on the International Space Station. Using the JEM-EUSO telescope an elaborate air fluorescence telescope with super-wide field of view, we aim at surpassing the existing and planned EECR detector in exposure by an order of magnitude. Observing from the space avails the observation principle of small ambiguity in thanks to distinct fluorescence and Cherenkov photons from extensive air showers (EASs) at nearly constant distances. The air shower simulations indicate that the advantage of space-based observation is solid against poorly known nature on primary EECRs and their interactions.**

***Keywords*: JEM-EUSO Mission. Extreme energy cosmic rays. International Space Station.**

I. Introduction

JEM-EUSO (Extreme Universe Space Observatory on-board Japanese Experiment Module) is a new type space-borne observatory for extreme energy cosmic rays (EECR) [1]. The JEM-EUSO telescope will be accommodated on the Japanese Experiment Module / Exposed Facility (JEM/EF) of the International Space Station (ISS) at an orbit altitude— $H_{\rm orbit} \sim 400$ [km]. The scientific objective is to innovate astronomy and astrophysics through EECR channel and other exploratory objectives [2], [3], [4]. The origin and existence of EECRs (extreme energies referred to as $E_0 \sim 10^{20}$ eV and higher) remain an open puzzle in contemporary astroparticle physics [5]. To solve it in spite of notably small fluxes, the observation of more than 1000 EECRs above $\sim 7 \times 10^{19}$ eV, in other words megalinsley-scale exposure is highly required (1[linsley]= 1 [km^2 yr sr]).

Aiming at launching the telescope in 2013, the Phase-A study of the JEM-EUSO mission is conducted to first achieve all those critical requirements in the following five years operation. By means of air fluorescence technique, the observation is based on the indirect observation of extensive air showers (EASs) initiated by primary EECRs. This technique has been developed in the ground-based experiments, however, never been practiced in space experiment so far. Operated on the orbit, there are advantages in measurement and scientific merits. The distance to EASs is so constrained that the correction of light absorption may be limited. Also thanks to an orbit inclination of 51.6°, the overall operations will cover the entire celestial sphere that enables to discover, and if positive then to identify and to study, EECR source objects in any celestial location.

In the following, we present the basic principle of the EECR observation principle in the JEM-EUSO mission. Using air shower simulations, we also discuss the key shower properties relevant to the observation method.

II. Apparatus overview

In this section we briefly describe an overview of the apparatus. The JEM-EUSO telescope has been space-qualified designed to achieve scientific objectives that define the basic requirements for the telescope and other subsystems. Here we focus on key parameters relevant to EAS measurements. Details on other subsystems may be referred in [6] and references therein.

The JEM-EUSO telescope has an aperture of ~ 4.5 m^2 viewed by the set of the 'photo-detector modules' (PDMs). The optical system consists of two curved double Fresnel lenses and a flat precision Fresnel lens [7]. The focal surface is aspherically curved and is covered by about 150 PDMs [8]. Each PDM is composed of a set of 36 $(= 6 \times 6)$ multi-anode photomultipliers (MAPMTs) with ultra-bialkali photocathode [9] or of silicon photomultipliers [10] as an alternative advanced option. PDMs are aligned to minimize the dead space.

In the baseline design, about 5000 MAPMTs are deployed in total. The field of view (FOV) is as super-wide as $\sim 60°$. Each MAPMT has a 6×6-pixel array and the total number of pixels is about 2×10^5. The spatial resolution corresponds to $\sim 0.1°$. For the nominal $H_{\rm orbit} \sim 400$ [km], the observation area is $\sim 2 \times 10^5$ km^2 with an ~ 750 m resolution on the Earth's surface. The time resolution is optimized to 2.5 μs which we call gate time unit (GTU) for trigger algorithm [11] and data acquisition scheme [12] for EAS observation.

III. Observation principle

In the JEM-EUSO mission, the observation and reconstruction of EECRs are based upon the measurements of EAS phenomenon induced by the primary particle incident in the atmosphere. By the JEM-EUSO telescope on the orbit, EAS events are observed as a luminous spot that moves at the speed of light. An actual reconstruction methods may be referred in [13].

Fig. 1 illustrates the EECR observation principle in the JEM-EUSO mission. At $H_{\rm orbit} \sim 400$ km, the JEM-EUSO telescope monitors transient luminous phenomena in an huge area of ~ 250 km radius. The main

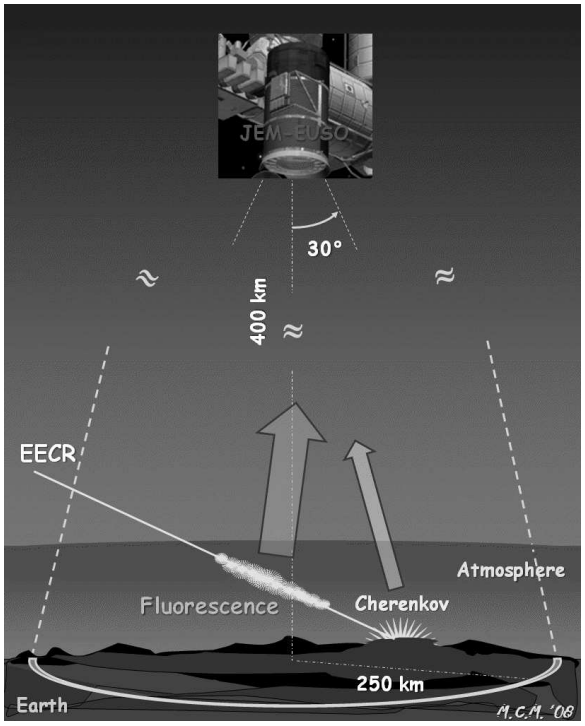

Fig. 1. Illustration of EECR observation principle in the JEM-EUSO mission. For the telescope at $H_{\rm orbit} \sim 400$ km altitude, the main signals are fluorescence photons along the EAS track and Cherenkov photons diffusely reflected from the Earth's surface.

signals from the EAS are fluorescence light and diffusely reflected Cherenkov light by the Earth's albedo.

For JEM-EUSO as a space-based fluorescence telescope, a huge volume of the atmosphere in FOV is itself a part of the giant 'detector.' For example, a primary 10^{20} eV EECR incoming to such volume produces an order of 10^{11} particles at maximum as a result of subsequent interactions in EAS. Secondary particles are still relativistic and the charged particles, most dominantly electrons, excite the nitrogen atoms to emit ultraviolet (UV) fluorescence light of characteristic lines in wavelengths $\lambda \sim 330 - 400$ [nm]. The total yield has been intensively studied by many groups and evaluated to be ~ 4 photons m^{-1} per electron [14]. Along the development of an EAS of this energy, an order of 10^{15} photons are isotropically emitted. At ~ 400 km distance, the solid angle of the telescope aperture is $\sim 2 \times 10^{-12}$ sr and therefore an order of thousands of photons direct toward the telescope.

Fig. 2 shows the transmittance of upward photons as a function of emission altitude. The curve denotes the average for photons ($\lambda = 300 - 400$ [nm]) from EASs. For evaluation, we used the software package ESAF (Euso Simulation and Analysis Framework) [15] that employs the LOWTRAN atmospheric model [16]. For reference of relevant altitudes of ESA development, the gray-scale stripes represent the number of charged particles— $N_{\rm charged}$ in the EAS by proton with $E_0 = 10^{20}$ eV from zenith angles— $\theta \sim 30^\circ, 60^\circ, 85^\circ$.

From the JEM-EUSO telescope at $H_{\rm orbit} \sim 400$ [km],

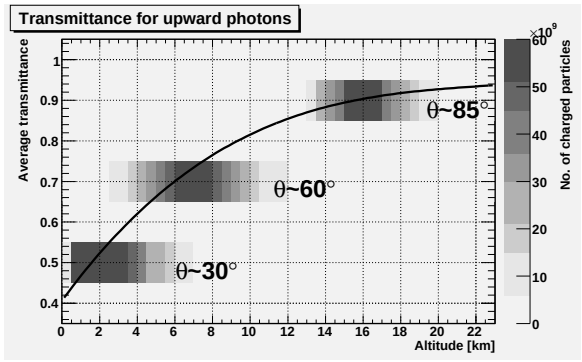

Fig. 2. Transmittance for upward photons as a function of altitude. The curve denotes the average for photons from EASs over $\lambda = 300-400$ [nm] band from EASs. For reference of EAS developing altitudes, the gray-scale stripes represent $N_{\rm charged}$ in the EAS from proton with $E_0 \sim 10^{20}$ eV from different θ.

the distance little varies to most EASs of interest that develop below the lower stratosphere (~ 20 km altitude). This fact reduces uncertainty in correction factor (~ 3 at maximum) for light attenuation in the atmosphere. Compared to ground-based experiments with limited FOV, they observe photons from EASs at variety of distances in most cases through aerosol-rich atmosphere.

It is worthy noting that the large FOV allows to look at the stage of the EAS development where most of fluorescence light is emitted until the EAS is fully attenuated for large θ or it reaches the Earth's surface. Unlike often case with ground-based telescopes, the profile of the EAS development is estimated without extrapolating the data to out of FOV. It is especially important for the EASs from large θ or gamma ray induced EASs that develop with longer durations [3].

To demonstrate how typical EASs are observed by the JEM-EUSO telescope, we present the case for the proton with $E_0 = 10^{20}$ eV and $\theta = 60^\circ$ with an impact position at 125 km off the center of FOV. The EAS was simulated with the air shower simulation code CONEX [17] for generation and the ESAF for emission and transport of photons in the atmosphere. Fig. 3 shows the arrival time profile (per GTU = 2.5 [μs]) of photons from the typical EAS event to the pupil of the JEM-EUSO telescope. The open histogram represents all photons and the fluorescence component is distinguished by the shaded histogram.

Fig. 4 shows the track image of the same typical EAS on the focal surface detector. The time-integrated signal in each pixel is denoted in digitalized scale. The small blocks correspond to MAPMTs. The arrow indicates the direction of movement of the signals.

In reality, there exist various background sources in the sensitive UV band. The reference level of the background noise from natural sources is ~ 500 photons m^{-2} ns^{-1} sr^{-1} that yields an order of 1–2 photoelectrons per GTU in each pixel. In events of an EAS, signals in the time-space frame are extracted by the pattern recognition techniques [13]. This also determines the

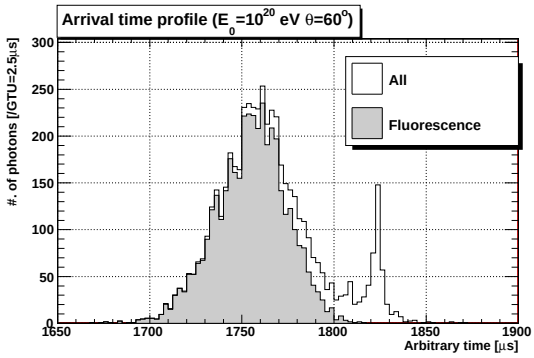

Fig. 3. Arrival time profile of photons from a typical EAS event to the JEM-EUSO telescope. The open histogram shows the number of photons arrival to the JEM-EUSO optical pupil. The shaded histogram represents of fluorescence component.

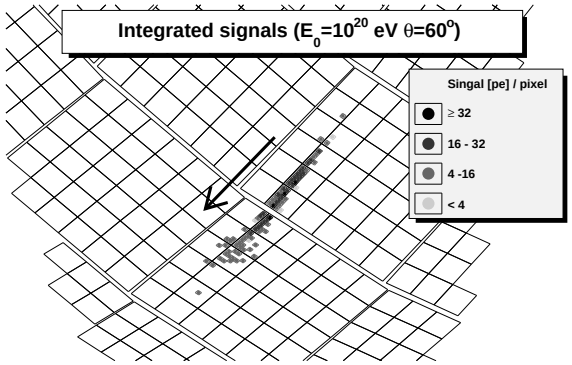

Fig. 4. Image on the focal surface detector for the same typical EAS as in Fig. 3. The time-integrated signal in each pixel is shown in digitized scale. The blocks correspond to the individual MAPMTs. The arrow indicates the direction of the movement of the signals.

so-called shower-detector-plane. The θ of EASs may be determined by the angular velocity of EAS light spot.

For EAS measurement on the orbit, fluorescence photons are dominant signal component whose intensity is almost proportional to the number of particles. The E_0 of EECRs may be estimated by the number of electrons— $N_{\max}$ or by the calorimetric approach (see further discussion in the next section).

Some Cherenkov photons also reach the telescope which consists of two components— scattered in the atmosphere; and reflected from the Earth's surface or from the optically thick clouds. Due to short-λ-dominant emission spectrum, Cherenkov photons are strongly suppressed in both downward and upward paths to the telescope by Rayleigh scattering and absorption by ozone.

Survived Cherenkov photons are still potential source of uncertainty in E_0 estimation. Observing from the space, however, the scattered component is not significant in EAS developing stage at higher altitudes. At lower altitudes where EAS attenuates, the Cherenkov photons turn dominant in the signal on the telescope. These photons have propagated downward with the so-called 'Cherenkov angle' ($\sim 1.4^\circ$ on the Earth's surface) and therefore broadly distribute beyond the intrinsic EAS spread. But their arrival time tends to be coherent and separated from the main EAS part. Such peaking helps locate the impact point on the Earth's surface.

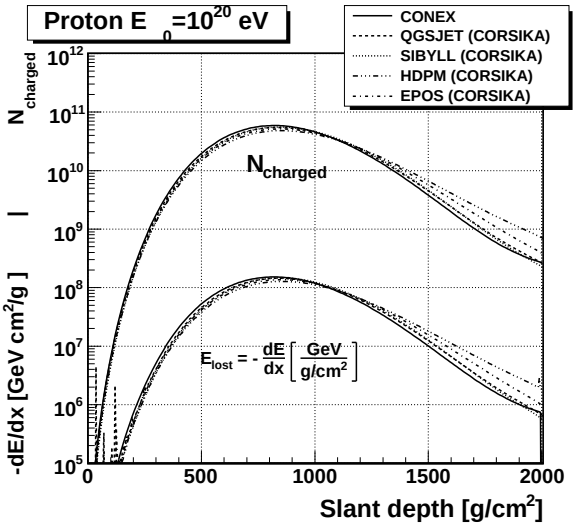

Fig. 5. $N_{\rm charged}$ and ionization loss $-dE/dX$ as a function of slant depth for the EAS from a 10^{20} eV proton. The solid curves denote the result by CONEX with QGSJET-II and the other curves with CORSIKA coupled with different high energy interaction models (QGSJET-II, SIBYLL, EPOS and HDPM) by curves as in the legend.

IV. Extensive air shower simulations

The EAS phenomenon is the basis of the observation principle even though the uncertainty could be arisen by poorly known nature of EECR species and interactions in EAS. In this section, we discuss the stability of the observation method using the air shower simulations. Unless otherwise mentioned, we used the CONEX code incorporated with high energy hadronic interaction model of QGSJET-II [18]. CONEX allows very fast generations of EASs by a hybrid approach with full Monte Carlo method in the early stage of development followed by numerical solutions of cascade equations. For comparison with better accuracies, we also simulated with the CORSIKA code [19] in particular case.

Fig. 5 shows the summary of the simulated result of EAS development for 10^{20} eV proton. As a function of slant depth, the number of charged particles $N_{\rm charged}$ (upper curves) and ionization loss $-dE/dX$ in unit of GeV per g/cm^2 (lower) are drawn. The solid curves denote the result from CONEX with QGSJET-II. Results from CORSIKA using different high energy interaction models (QGSJET-II, SIBYLL [20], HDPM [21] and EPOS [22]) are also given by curves as in the legend.

Conservatively speaking, when $N_{\rm charged}$ is larger than $\sim 10^9$, more than ~ 100 photons per GTU are expected to arrive to the JEM-EUSO telescope at nominal $H_{\rm orbit}$. In such a case signals are clearly significant against background noise. For EASs above $\sim 10^{19}$ eV, this criterion is well satisfied in the effective part of development to infer basic EAS parameters, i.e. E_0, direction and $X_{\max}$. Over this part, the ratio of $-dE/dX$ to

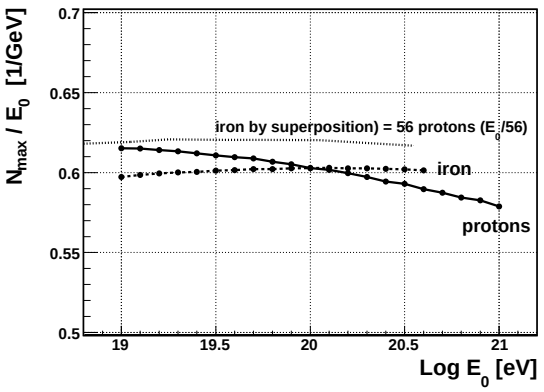

Fig. 6. Ratio of $N_{\max}$ to E_0 as a function of E_0 for proton (solid curve) and iron (dashed) induced EASs. For comparison, the relation for iron by simple superposition model is drawn by the dotted curve.

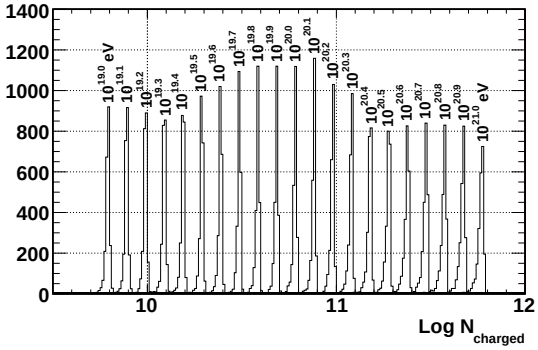

Fig. 7. $N_{\max}$ distributions for EASs from proton of $E_0 = 10^{19}, 10^{19.1}, \ldots, 10^{21}$ [eV] indicated by figures.

$N_{\rm charged}$ is nearly constant independent of interaction models assumed. This ensures, with proper analysis, the validity of $N_{\rm charged}$ estimation from the fluorescence light measurement.

Fig. 6 shows the ratio of $N_{\max}$ to E_0 as a function of E_0 for proton (solid curve) and iron (dashed) induced EASs. For comparison, the relation for iron assuming simple superposition model is drawn by dotted curve.

Fig. 7 shows $N_{\max}$ distributions for EASs from proton of $E_0 = 10^{19}, 10^{19.1}, \ldots, 10^{21}$ [eV].

$N_{\max}$ is one of known energy estimators, which is almost proportional to E_0 weakly depends upon primaries. Comparing the tested models in Fig. 6, the uncertainty in $N_{\max}$ is $\sim 10\%$. As seen in Fig. 7, intrinsic fluctuations of $N_{\max}$ are far smaller than other uncertainties.

Fig. 8 shows the ratio of total energy loss of all particles to E_0 as a function of E_0 as same as in Fig. 6.

It is widely accepted that the total energy deposit may indicate almost E_0 on basis of calorimetry. The result indicates $> 95\%$ energy deposited through the EAS development. The rest is the so-called missing energy by muons and neutrinos that account for very little dependence on models or primaries. This method is a natural approach for the JEM-EUSO telescope that is capable of measuring the EAS development in wide range as already motioned.

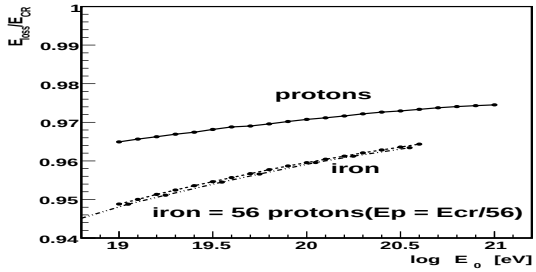

Fig. 8. Same as Fig. 6 but ratio of total energy loss of all particles to E_0 as a function of E_0.

V. SUMMARY

The JEM-EUSO mission aims at EECR observing on the ISS orbit using an elaborate fluorescence telescope with super-wide FOV. As well as expected a huge observation area, the simple geometry between EASs and the telescope enables to determine the fundamental EAS parameters with little uncertainty. Despite of lack of knowledge of interaction models, the air shower simulations indicate that the stability of the observation principle is solid. The sophisticated studies for analysis of EAS observations are ongoing and some results will be presented in the present Conference.

ACKNOWLEDGMENT

The part of the present work is obtained by the ESAF software package [15] that had been developed by ESAF Developers Team since the Phase-A study of the EUSO mission conducted under the European Space Agency initiative. KS wishes to thank for their hospitality in Andrzej Soltan Institute for Nuclear Studies, Institut für Astronomie und Astrophysik Tübingen, Germany and Joint Institute of Nuclear Research, Russia where the most part of present work was performed.

REFERENCES

[1] T. Ebisuzaki *et al.*, Nucl. Phys. B (Proc. Suppl.) 175, 237 (2008).
[2] G. Medina-Tanco *et al.*, in these proceedings (2009).
[3] A.D. Supanitsky *et al.*, in these proceedings (2009).
[4] A.D. Supanitsky *et al.*, in these proceedings (2009).
[5] For review, S. Petrera, (preprint) arXiv:0810.4710v2 [astro-ph], (2008).
[6] F. Kajino *et al.*, in these proceedings (2009).
[7] Y. Takizawa *et al.*, in these proceedings (2009).
[8] Y. Kawasaki *et al.*, in these proceedings (2009).
[9] Y. Kawasaki *et al.*, Nucl. Instr. and Meth. A564, 378 (2006).
[10] H. Miyamoto *et al.*, in these proceedings (200).
[11] O. Catalano, in these proceedings (2009).
[12] M. Casolino, in these proceedings (2009).
[13] T. Mernik *et al.*, in these proceedings (2009).
[14] For review, F. Arqueros *et al.*, Nucl. Instr. Meth. A597, 1 (2009).
[15] A. Thea *et al.*, Proc. of 31st Int. Cosmic Ray Conf. (Pune), 8, 133 (2005).
[16] F.X. Kneizys, AFGL-TR-0177, U.S. Air Force Geophysics Laboratory, Hanscom (1988).
[17] T. Bergmann *et al.*, Astropart. Phys. 26, 420 (2007).
[18] S. Ostapchenko, Phys.Rev. D 74, 014026 (2006).
[19] D. Heck *et al.*, FZKA Report-6019, ed. Forschungszentrum Karlsruhe (1998).
[20] R. Engel *et al.*, Proc. 26th Int. Cosmic Ray Conf. (Salt Lake City), 1, 415 (1999).
[21] J.N. Capdevielle, J. Phys. G: Nucl. Part. Phys. 15, 909 (1989).
[22] K. Werner *et al.*, Phys. Rev. C, 74, 044902 (2008).